Origin of enantioselectivity in palladium-catalyzed asymmetric allylic alkylation reactions using chiral N,N-ligands with different rigidity and flexibility†

Dario Drommi,*[a] Maria Saporita,[a] Giuseppe Bruno,[a] Felice Faraone,*[a] Patrizia Scafato[b] and Carlo Rosini[b]

Received 18th December 2006, Accepted 22nd February 2007
First published as an Advance Article on the web 9th March 2007
DOI: 10.1039/b618347f

The chiral bidentate-N,N ligands, (S_a)-**1**, (S_a)-**2**, (*S*,*S*)-**3** and (*S*,*S*)-**4**, were synthesized. They were shown to contain rigid 2-pyridinyl or 8-quinolinyl building blocks and the C_2-symmetric chiral frameworks *trans*-2,5-dimethylpyrrolidinyl or (*S*)-(+)-2,2′-(2-azapropane-1,3-diyl)-1,1′-binaphthalene. In the (S_a)-**2**, and (*S*,*S*)-**4** ligands pair, the 8-quinolinyl skeleton is directly bonded to the C_2-symmetric chiral frameworks (*S*)-(+)-2,2′-(2-azapropane-1,3-diyl)-1,1′-binaphthalene or *trans*-2,5-dimethylpyrrolidinyl. This feature induces rigidity in this pair of ligands upon the N,N-framework. However, this does not occur for the (S_a)-**1** and (*S*,*S*)-**3** ligands, in which the presence of the $-CH_2-$ spacer between the frameworks bearing the nitrogen atom donors gives greater flexibility to the ligand. A further difference between the pairs of ligands is significant from the electronic properties of the chiral framework N-donor atom. The coordinating properties and the specific steric structural features of the (S_a)-**1**, (S_a)-**2**, (*S*,*S*)-**3**, and (*S*,*S*)-**4** ligands are explained by their reactions with the $[Pd(PhCN)_2Cl_2]$ and $[Pd(\eta^3\text{-PhCHCHCHPh})(\mu\text{-Cl})]_2$ substrates, in which the reported ligands form chelate complexes, with the exception of (S_a)-**2**, which failed to react with $[Pd(\eta^3\text{-PhCHCHCHPh})(\mu\text{-Cl})]_2$. The ligands were used in the palladium–allyl catalyzed substitution reaction of 1,3-diphenylallyl acetate with dimethylmalonate, with the best result being obtained using the (S_a)-**1** ligand, giving the substitution product 2-(1,3-diphenylallyl)dimethylmalonate with an enantiomeric excess of 82% in the *S* form and a yield of 96%. The work demonstrates that in the presence of a steric ligand control, the electronic properties of the ligand donor atoms play a role though not significant in determining the enantioselectivity of palladium(II) catalyzed allylic substitution reactions. The results of the catalytic reaction do not provide a convincing explanation considering the coordinated chiral ligand features, as rigidity or flexibility and electronic properties of the N-donor atoms. A rationalization of the results is proposed on the basis of NMR studies and DFT calculation on the cationic complexes $[Pd(\eta^3\text{-PhCHCHCHPh})(\text{N-N}^*)]CF_3SO_3$, (N-N* = ($S_a$)-**1**, **9**; (*S*,*S*)-**3**, **10**; (*S*,*S*)-**4**, **11**).

Introduction

Enantioselective palladium(II)-catalyzed allylic substitution reactions are among the most studied reactions aimed at determining carbon–carbon bond formation between allylic substrates and carbon nucleophiles.[1] Steric and electronic chiral chelating ligand features were exploited to recognize factors, which enhance differentiation between enantiotopic allyl carbon atoms, in the cationic palladium(II)–allyl catalytic species, and direct nucleophilic attack to afford the substitution product in high yield and enantiomeric excess. These studies also allowed the establishment of the reaction steps in which the enantioselectivity of the process can be determined. Chiral chelating ligand classes which have been found to induce efficiency in the catalytic system include P-N and N-N donors,[2,3] planar-chiral ferrocenyl derivatives[4] and dissymmetric diphosphines.[5] The rigidity and the flexibility of the chiral chelating ligand involved in the catalytic species, $[Pd(\eta^3\text{-PhCHCHCHPh})(\text{N-N}^*)]^+$ (N-N* = chiral chelating ligand), have been considered important features in the design of the catalyst, even if these properties may often give ambiguous indications. This study reports the use of two pairs of chiral N-N-chelating ligands in conventional palladium-catalyzed asymmetric allylic alkylation reactions; they contain rigid 2-pyridinyl or 8-quinolinyl building blocks and the C_2-symmetric chiral frameworks (*S*)-(+)-2,2′-(2-azapropane-1,3-diyl)-1,1′-binaphthalene) or *trans*-2,5-dimethylpyrrolidinyl (Fig. 1). The pairs of ligands differ from each other in the sp^2 or sp^3 carbon atom spacer of the N-donor arms (in each ligand the two N-donor arms are different) and in the basic electronic properties of the N-donor atom of the chiral framework. The aim of the study was to gain insight into the effects of ligand properties, such as the rigidity or flexibility of the chiral chelating ligand and the influence of the donor-atoms, in determining asymmetric induction in the catalytic process and namely, to establish the relation between regioselectivity induced

[a]*Dipartimento di Chimica Inorganica, Chimica Analitica, Chimica Fisica dell'Università di Messina, Salita Sperone 31, Vill. S. Agata, 98166, Messina, Italy. E-mail: faraone@chem.unime.it.*
[b]*Dipartimento di Chimica dell'Università della Basilicata, 85100, Potenza, Italy*

† Electronic supplementary information (ESI) available: Experimental data, spectral characterization, and DFT calculation table. See DOI: 10.1039/b618347f

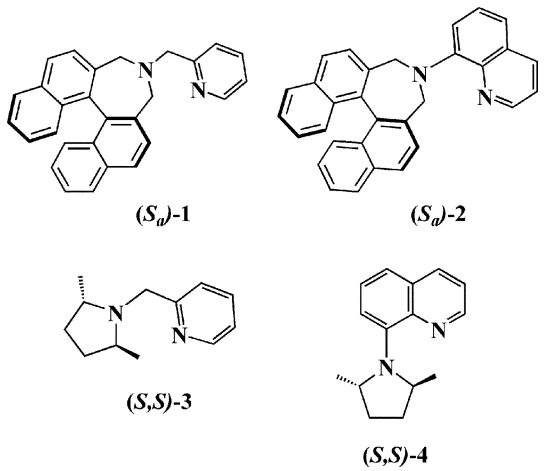

Fig. 1 Used chiral ligands.

by the chelated chiral ligands in the catalytic process involving each conformational isomer present in solution and the enantiomeric excess of the obtained product. The here reported chiral bidentate-N,N ligands, (S_a)-**1**, (S_a)-**2**, (*S*,*S*)-**3**, and (*S*,*S*)-**4** (Fig. 1), include both of the nitrogen donor atoms in a heterocyclic ring.

The (S_a)-**1** ligand had been previously prepared by one of us.[6](*S*,*S*)-**3** was briefly described[7] but its application in metal-catalyzed asymmetric synthesis has not been explored in detail. In the (S_a)-**2**, and (*S*,*S*)-**4** ligands, the 8-quinolinyl skeleton was found to directly bind to the C_2-symmetric chiral frameworks (*S*)-(+)–2,2′-(2-azapropane-1,3-diyl)-1,1′-binaphthalene or *trans*-2,5-dimethylpyrrolidinyl; these features induce rigidity in the N,N-framework of this pair of ligands. However, no such properties were observed for the (S_a)-**1** and (*S*,*S*)-**3** ligands, in which the presence of the –CH_2– spacer between the frameworks bearing the nitrogen atom donors gives more flexibility to the ligands. A further observed difference between the pairs of ligands concerns the electronic properties of the chiral framework N-donor atom. In the (S_a)-**1** and (*S*,*S*)-**3** pair, the basicity of the chiral framework N-donor atom was evaluated as being considerably higher than that of (S_a)-**2** and (*S*,*S*)-**4** pair.[8] We also examined the coordinating properties of the synthesized ligands toward palladium(II) substrates obtaining information by a detailed multinuclear NMR study about the major conformational isomers [Pd(η^3-PhCHCHCHPh)(N-N*)]$^+$present in solution, their concentration ratio and the existence of exchange processes. Theoretical DFT calculations on the relative stability and the simulated structure of the cationic catalytic species [Pd(η^3-PhCHCHCHPh)(N-N*)]$^+$of conformational isomers is also reported. Previously,[9] we yielded several reports focusing on the effect of the coordinated ligand features in determining the enantiomeric excess in the allylic alkylation palladium-catalyzed process.

Results

Synthesis of the chiral ligands

(S_a)-**1** and (S_a)-**2** ligands were obtained by reacting (*S*)-(+)-2,2′-bis-bromomethyl-1,1′-binaphthalene with 2-aminomethylpyridine or 8-aminoquinoline respectively, in a 1 : 6 molar ratio in THF under reflux conditions. (S_a)-**1** and (S_a)-**2** ligands were purified by chromatography and obtained as white and yellow solids, respectively. They are found to be stable in the air, at room temperature, for a long time. (*S*,*S*)-**3** and (*S*,*S*)-**4** ligands were obtained by the reaction of (2*R*,5*R*)-2,5-hexanediol cyclic sulfate with 2-aminomethylpyridine or 8-aminoquinoline, respectively, in a molar ratio of 1 : 1.86 in THF solution under reflux. n-BuLi was added to the resulting precipitate, indicating the presence of the corresponding Zwitterionic amine-sulfate species, and the mixture was refluxed for 72 h. (*S*,*S*)-**3** was obtained as a yellow oil while (*S*,*S*)-**4** was in the form of a yellow crystalline solid. The (S_a)-**1**, (S_a)-**2**, (*S*,*S*)-**3** and (*S*,*S*)-**4** ligands were characterized by elemental analysis and ^{1}H NMR spectroscopy (see Experimental section).

Reactions of (S_a)-1, (S_a)-2, (*S*,*S*)-3 and (*S*,*S*)-4 ligands with [Pd(PhCN)$_2$Cl$_2$] and [Pd(η^3-PhCHCHCHPh)(μ-Cl)]$_2$

To gather information about the coordinating properties and the specific structural features of the (S_a)-**1**, (S_a)-**2**, (*S*,*S*)-**3** and (*S*,*S*)-**4** ligands, we explored their reactions with [Pd(PhCN)$_2$Cl$_2$] and palladium(II)–allyl substrate [Pd(η^3-PhCHCHCHPh)(μ-Cl)]$_2$.

The reactions with [Pd(PhCN)$_2$Cl$_2$] were carried out at room temperature in CH_2Cl_2 solution in a 1 : 1.2 complex : ligand ratio. The products, [Pd(N-N*)Cl$_2$], **5**–**8**, (N-N*= (S_a)-**1**, **5**; (S_a)-**2**, **6**; (*S*,*S*)-**3**, **7**; and (*S*,*S*)-**4**, **8**), were obtained in almost quantitative yields as yellow solids by precipitation from CH_2Cl_2–hexane; which later underwent elemental analysis and ^{1}H NMR spectroscopy.[10]

The cationic complexes, [Pd(η^3-PhCHCHCHPh)(N-N*)]CF_3SO_3, (**9**–**11**) (N-N*= (S_a)-**1**, **9**; (*S*,*S*)-**3**, **10**; and (*S*,*S*)-**4**, **11**), which are the catalytic species in the allylic substitution reaction, were synthesized by the reaction of [Pd(η^3-PhCHCHCHPh)(μ-Cl)]$_2$ with a stoichiometric amount of the N-N*-chiral ligand, in CH_2Cl_2 solution, and, subsequently, after 1 h, with solid $AgCF_3SO_3$. Filtration through Celite and evaporation of the solvent yields a solid product, which was recrystallized using CH_2Cl_2–hexane. The (S_a)-**2** ligand failed to give the corresponding cationic complex [Pd(η^3-PhCHCHCHPh)((S_a)-**2**)]CF_3SO_3, but it reacted easily with [Pd(η^3-H_2CCHCH$_2$)Cl]$_2$, in the absence of phenyl-substituents on terminal allylic carbon atoms, to give [Pd(η^3-H_2CCHCH$_2$)((S_a)-**2**)]CF_3SO_3, **12**.

The compounds **9**–**11** were characterized by elemental analysis, conductivity measurements and spectroscopic multinuclear NMR studies; these will be widely discussed in later sections. The experimental data allowed us to establish that (S_a)-**1**, (S_a)-**2**, (*S*,*S*)-**3** and (*S*,*S*)-**4** ligands act, in the compounds **5**–**11**, as chelating ligands leading to a square planar geometry.[10] Unfortunately, crystals of compounds **9**–**11** suitable for X-ray analysis could not be obtained.

NMR Studies

In the ^{1}H NMR spectra of **5**–**8**, the shift of the N-N* ligand signals indicates their coordination to the palladium centre. For example, in the ^{1}H NMR spectra of [Pd((S_a)-**1**)Cl$_2$], **5**, and [Pd((*S*,*S*)-**3**)Cl$_2$], **7**, the pyridine *ortho*-hydrogen was observed to shift downfield. The same shift of the *ortho*-hydrogen signal of the quinoline framework was observed in the ^{1}H NMR spectra of [Pd((S_a)-**2**)Cl$_2$], **6**, and [Pd((*S*,*S*)-**4**)Cl$_2$], **8**. However, a different effect was

noted for the cationic complexes [Pd(η^3-PhCHCHCHPh)((S_a)-**1**)]CF_3SO_3, **9**, [Pd(η^3-PhCHCHCHPh)((*S*,*S*)-**3**)]CF_3SO_3, **10**, and [Pd(η^3-PhCHCHCHPh)((*S*,*S*)-**4**)]CF_3SO_3, **11**, in which the *ortho*-hydrogen lies at an upfield chemical shift due to the ring current effect of the *cis* phenylic substituent in the allylic moiety (see below). As expected, the signals of diastereotopic CH_2-hydrogens further split due to ligand chelation.

In order to gain information about the conformational isomers of compounds **9–11** present in solution and their concentration ratio, we undertook a multinuclear NMR study. Fig. 2 shows the possible conformational isomers for a cationic species such as [Pd(η^3-PhCHCHCHPh)(N-N*)]$^+$, indicating the nomenclature and the symbols used for the allyl-carbon atoms and the adopted atoms numeration.[11]

Furthermore, it was delineated that in solution, the different conformations can be in equilibrium and may give rise to exchange processes.[12] Thus, preliminarily to a catalytic test, it was very useful to have knowledge about the allylic conformational isomers present under the catalytic conditions and to retrieve information about the possible steric or electronic effects, which determine the site of nucleophilic attack.[13,14] As far as the asymmetric C_2-chiral bidentate ligands (S_a)-**1**, (S_a)-**2**, (*S*,*S*)-**3** and (*S*,*S*)-**4**, are concerned, they exhibit a chiral framework on the more basic and more sterically demanding nitrogen atom; it is clear that their coordination to the palladium(II) centre modifies differently the electronic features of terminal allylic carbon atoms and induces a desymmetrization of the allyl moiety. As pointed out above, in the (S_a)-**1** and (*S*,*S*)-**3** ligands, the basicity of the chiral framework N-donor atom is of *ca.* five pK_a units higher than that of (S_a)-**2** and (*S*,*S*)-**4**.[8]

In a typical experiment, a weighed amount of any species Pd(η^3-PhCHCHCHPh)(N-N*)CF_3SO_3, **9–11**, is dissolved in $CDCl_3$, in the NMR tube. When equilibrium is reached, the conformational isomers present in solution are detected by ^{1}H, and ^{13}C NMR spectroscopy. A combination of ^{1}H COSY, ^{13}C, ^{1}H heteronuclear correlation (HMQC), and 2D NOESY experiments is used to ascertain the allylic arrangement in the conformational isomers and the related structures in solution. Relevant ^{1}H and ^{13}C NMR data are summarized in Table 1.

The 1,3-diphenylallyl cationic complex [Pd(η^3-PhCHCHCHPh)((S_a)-**1**)]CF_3SO_3, **9**, exists in $CDCl_3$ solution as a mixture

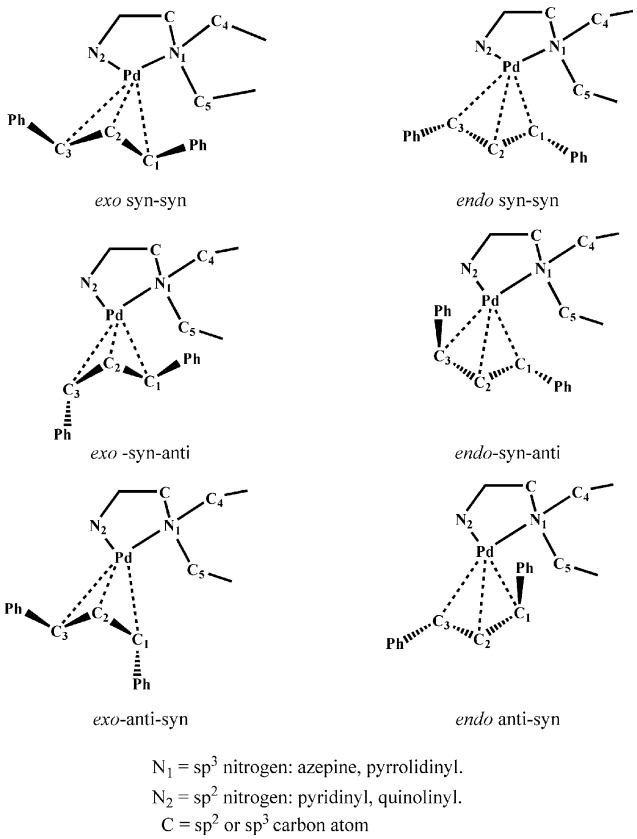

Fig. 2 Possible allyl–palladium conformational isomers and adopted atoms numeration.

of two prevalent isomers, the *endo-syn-syn*, **9a**, and the *exo-anti-syn*, **9b**, in an *ca.* 70 : 30 ratio (Fig. 3). The NMR spectra failed to clearly show the presence of the *exo-syn-syn* conformational isomer in solution, that is normally considered on the basis of the DFT calculation, the conformer, at lowest energy, together with *endo-syn-syn*.[3g] The 2-D exchange spectra indicate that the **9a** and **9b** isomers exchange at room temperature with a η^3:η^1:η^3 mechanism, on the NMR time-scale.[12] Selective NOEs between the allyl protons and the proximate ligand protons allow the

Table 1 Selected ^{1}H and ^{13}C NMR data for complexes **9–11**[a,b]

	H_1	H_2	H_3	C_1	C_3	
endo-syn-syn-**9** (**9a**)	4.33	6.48	4.95	78.3	77.5	7.48 (d, 1H, H_{opy}) 4.72 (d, 1H, ^2J 15 Hz, CH_2, 4a), 4.08 (d, 1H, ^2J 12 Hz, CH_2, 5a), 3.70 (d, 1H, ^2J 15 Hz, CH_2, 4b), 3.35 (d, 1H, ^2J 14 Hz, CH_2, 6a), 2.89 (d, 1H, ^2J 12 Hz, CH_2, 5b), 2.35 (d, 1H, ^2J 14 Hz, CH_2, 6b)
exo-anti-syn-**9** (**9b**)	5.38	6.35	4.84	85.1	73.2	7.53 (d, 1H, H_{opy}), 5.47 (br, 1H, CH_2, 4a), 4.27 (br, 1H, CH_2, 5a), 3.69 (br, 1H, CH_2, 4b), 3.44 (br, 1H, CH_2, 6a), 2.95 (br, 1H, CH_2, 5b), 2.64 (br, 1H, CH_2, 6b)
exo-syn-syn-**10** (**10a**[d])	4.84	6.52	4.88	77.9	76.3	7.56 (d, 1H, H_{opy}), 4.48 (d, 1H, ^2J 15 Hz, CH_2, 4a), 3.73 (d, 1H, ^2J 15 Hz, CH_2, 4b), 2.73 (m, 1H, CH, 5), 2.28 (m, 1H, CH, 6), 1.44 (d, 3H, ^3J 7 Hz, CH_3), 1.01 (d, 3H, ^3J 7 Hz, CH_3)
endo-syn-syn-**10** (**10b**[d])	4.65	6.58	4.79	78.2	77.7	7.16 (d, 1 H, H_{opy}), 3.94 (d, 1H, ^2J 15 Hz, CH_2, 4a), 3.78 (d, 1H, ^2J 15 Hz, CH_2, 4b), 3.09 (m, 1H, CH, 6), 2.43 (m, 1H, CH, 5), 1.57 (d, 3H, ^3J 7 Hz, CH_3), 0.70 (d, 3H, ^3J 7 Hz, CH_3)
endo-syn-syn-**11** (**11a**)	5.10	6.57	5.14	79.0	83.4	7.79 (d, 1H, H_{opy}), 3.69 (m, 1H, CH, 5), 2.17 (m, 1H, CH, 6), 1.67 (d, 3H, ^3J 7 Hz, CH_3), 0.70 (d, 3H, ^3J 7 Hz, CH_3)
exo-syn-syn-**11** (**11b**)	5.08	6.64	5.19	78.8	75.9	7.48 (d, 1H, H_{opy}), 4.67 (m, 1H, CH, 6), 3.55 (m, 1H, CH, 5), 1.15 (d, 3H, ^3J 7 Hz, CH_3), 0.98 (d, 3H, ^3J 7 Hz, CH_3)

[a] Chemical shifts, δ, are reported in ppm. [b] In $CDCl_3$ solution. [c] Coupling constants are in Hz. [d] At 223 K.

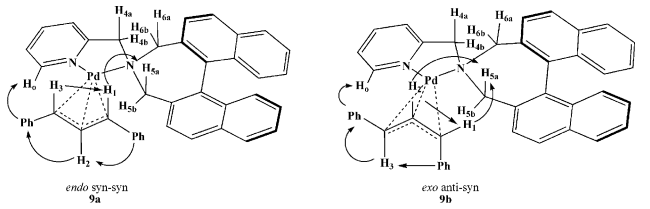

Fig. 3 Interpretation of NOESY data in determining the **9a** and **9b** isomers.

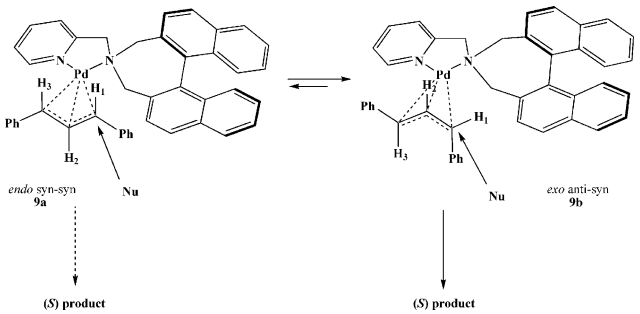

Fig. 4 Proposed transition state models for the asymmetric allylic substitutions in **9**.

distinction between the *endo-syn-syn* and *exo-anti-syn* isomers **9a** and **9b**, respectively. The major isomer exhibits an *endo-syn-syn* arrangement of the allyl unit, as shown by the coupling constants of 12 Hz between the terminal allylic protons H_3 and H_1 with the central H_2 proton. The strong NOE cross peak observed between the two terminal allylic protons H_3 and H_1 in **9a**, also supports the *syn-syn* configuration. The unambiguous assignment of the major isomer **9a** as *endo-syn-syn* is based on several critical NOE contacts (Fig. 3). For the *exo-anti-syn* isomer **9b**, all the signals are broad, also at lower temperatures, due to the exchange process with the isomer **9a**; the exchange obviously involves the isomer **9b** in minor population with a faster rate constant, *i.e.* a wider line-width. Its conformation was assigned considering the NOE contact shown in Fig. 3, and particularly the contact between H_2 and H_1 and especially the selective one between H_2 and a proton on the CH_2 group bonded to the N_1 nitrogen atom in the azepine fragment, since such NOE contact is not observed for the major isomer **9a**.

In both isomers, the chemical shift of the *ortho*-hydrogen of the pyridine moves to high field because it is affected by the resonance cone of the phenyl bonded to the allylic fragment.

A correlation between the ^{13}C NMR chemical shifts of the terminal allylic carbons and their electrophilicity, provided by the different *trans* influence of the chelating heteroatom donors and/or repulsive steric interaction of the substituents on the chelating donor atoms with the allylic carbon substituents, has been reported and used as a tool for predicting their reactivity.[13] In both isomers, **9a** and **9b**, the ^{13}C chemical shift values indicate that the terminal allyl carbons *trans* to the pyridinyl nitrogen atom are more deshielded (C_1 78.3 ppm for **9a** and 85.1 ppm for **9b**) than those *trans* to the chiral framework nitrogen atom (C_3 77.5 ppm for **9a** and 73.2 ppm for **9b**); this means that C_1 of both **9a** and **9b** would be more sensitive than C_3 towards nucleophilic attack. The weakening of the Pd–C_1 bond is enhanced due steric hindrance between the phenyl on the C_1 allyl carbon and the CH_2 group bonded to the nitrogen atom in the azepine fragment as shown by cross peaks in the 2D NOESY experiment (see also theoretical calculations section).

In addition, the increased downfield shift observed for C_1 of **9a** *versus* C_1 of **9b**, and the larger difference in the chemical shift between C_3 and C_1 in **9b** (*ca.* 12 ppm), compared to that observed for the same carbon atoms in **9a** (almost negligible, *ca.* 1 ppm), allow us to reason that **9b** is more reactive than **9a** towards nucleophilic attack at allylic carbon. All these data support the general model of the complex **9** proposed in Fig. 4, which shows nucleophilic addition occurring at an allyl carbon atom *trans* to the pyridinyl group consistent with the observed *S* absolute configuration of the allylic alkylation products.

Further positive cross peaks show that a mechanism exchange involves other minor isomers whose characterization was not possible due to their very low concentration and signal broadening. We do not exclude the fact that one of these minor isomers could be the *exo-syn-syn* conformer; as yet we are not able to explain its low concentration with the DFT calculations indicating a low energy difference between the *endo-syn-syn* and *exo-syn-syn* conformational isomers.

A different situation was found for the species **10** containing the (*S*,*S*)-**3** ligand. The 2D NOESY experiment, run at low temperature, made it possible to assign the configuration of the major isomers present in solution as *endo-syn-syn* (about 54%) and *exo-syn-syn* (about 42%) (see Fig. 5).

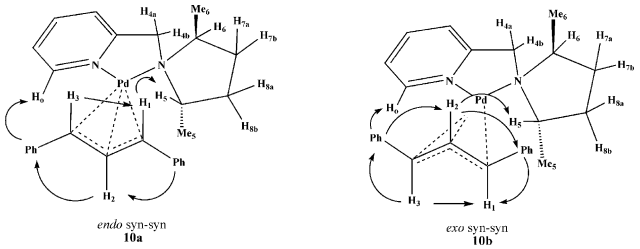

Fig. 5 Interpretation of NOESY data in determining **10a** and **10b** isomers.

Both the *endo-syn-syn* **10a** and *exo-syn-syn* **10b** species are involved in an exchange process, not between themselves, but with other minor isomers, as shown by a broadening of the proton signals at room temperature. In fact, all signals are broad at room temperature and we observed coalescence. By lowering the temperature to 223 K, all the signals sharpened except for the methyl and hydrogen protons close to the pyrrolidinyl nitrogen atom on account of undergoing a quick exchange and therefore they appeared broad. In this case, a steric hindrance between the phenyl on the allylic carbon atom and the CH_2 of the pyrrolidinyl group was observed; this is not able to occur with the methyl group that is free to move at low temperatures too. Under catalytic conditions, however, the nucleophile did not distinguish between the two terminal allyl-carbon atoms because at room temperature, the complex undergoes a fast exchange, determining the coalescence state.

The 2D NOESY experiment allowed the detection of [Pd(η^3-PhCHCHCHPh)((*S*,*S*)-**4**)]CF_3SO_3, **11**, with the configuration in solution of only two isomers in a greater amount as *endo-syn-syn* (67%), **11a**, and *exo-syn-syn* (29%), **11b**. For the other two

Table 2 Calculated (DFT) distances, angles and relative energies of **9–11**

	ΔE/kJ mol^{-1}	Pd–C_1/Å	Pd–C_3/Å	Pd–N_1/Å	Pd–N_2/Å	N_1–Pd–C_1/°	N_2–Pd–C_3/°
endo-syn-syn **9**	0	2.248	2.220	2.224	2.136	108.08	105.60
exo-syn-syn **9**	5.56	2.272	2.203	2.226	2.138	108.06	105.40
exo-anti-syn **9**	21.46	2.241	2.239	2.216	2.132	106.51	105.24
endo-syn-anti **9**	26.90	2.252	2.218	2.222	2.148	107.26	106.17
endo-syn-syn **10**	0	2.271	2.228	2.257	2.130	110.12	103.59
exo-syn-syn **10**	3.15	2.299	2.207	2.262	2.129	109.88	103.40
exo-anti-syn **10**	15.96	2.231	2.266	2.241	2.122	106.68	104.44
endo-syn-anti **10**	50.28	2.273	2.289	2.283	2.142	110.89	103.22
endo-syn-syn **11**	0	2.290	2.223	2.255	2.108	108.78	104.50
exo-syn-syn **11**	1.91	2.292	2.213	2.259	2.106	108.30	104.19
exo-anti-syn **11**	19.03	2.251	2.260	2.250	2.100	106.40	104.65
endo-syn-anti **11**	21.53	2.300	2.191	2.250	2.110	109.34	103.35

The N_1–Pd–N_2 and C_1–Pd–C_3 averaged bite angle values of the coordinated ligands and of the diphenylallyl-moiety coordination are 79.7° (78.0–80.8°) and 66.8° (65.4–68.6°), respectively.

isomers evidenced, it was not possible to establish an accurate configuration because they were found in low concentration and gave rather broad signals.

The two species **11a** and **11b** do not exchange in solution at 298 K temperature. The *syn-syn* configuration for the major isomers was assigned through the NOE peaks between the two allylic protons H_1 (5.14 ppm) and H_3 (5.10 ppm) for **11a** and H_1 (5.19 ppm) and H_3 (5.08 ppm) for **11b** and by the coupling constants of 12 Hz between the two terminal hydrogens and the central proton H_2. In both isomers, the chemical shift of the *ortho*-hydrogen of the quinoline shifted to high field because they are affected by the resonance cone of the allylic phenyl. The pyrrolidinyl ring hydrogens were in exchange due to the intramolecular axial–equatorial interconversion.

The terminal allylic carbon atoms C_1 signals of **11a** and **11b** are shifted to a lower frequency than the C_3 atoms because they were *cis* to the sterically bulky pyrrolidinyl group. The different electronic characteristics of the two isomers led to different chemical shifts for the two terminal allylic carbons (**11a**: 83.4 ppm, C_3; 79.3 ppm, C_1; **11b**: 79.2 ppm, C_3; 75.9 ppm, C_1); therefore the allylic carbon atoms exhibit a different behaviour and the two isomers give the product in a different conformation. The *endo-syn-syn* isomer was characterized by a higher chemical shift difference (4.1 ppm) between the two terminal allylic carbons than the *exo-syn-syn* isomer (3.3 ppm) present at minor concentration, and this, not being the isomers involved in an exchange process and not occurring under Curtin–Hammett conditions, may be the reason why the ee of the obtained products is not notable.

Theoretical calculations

Theoretical calculations have been performed on some conformational isomers of the cationic palladium(II)–allyl species [Pd(η^3-PhCHCHCHPh)(N-N*)]$^+$ (N-N*= (S_a)-**1**, **9**; (*S*,*S*)-**3**, **10**; (*S*,*S*)-**4**, **11**), to obtain information about their stability and structural features. The models used reproduce the features of the complete structures in a reliable way, namely the coordination environment of the palladium(II) centre and the chelate ring formed by the (S_a)-**1**, (*S*,*S*)-**3** and (*S*,*S*)-**4**, ligands. We performed DFT calculations on a molecule analogous to **9**, containing a biphenyl moiety instead of a binaphthyl one. Since the DFT calculations were applied to a static molecule, the difference between real binaphthyl species and the biphenyl-optimized model did not produce different results. We further verified that other phenylic groups present in the binaphthyl do not interact with phenyl-substituents on the palladium coordinated allyl moiety; in fact, the aforesaid groups are directed towards the less congested region of the cationic species. The observed geometrical parameters reported in Table 2, because of basis-set used (SDD) in the DFT calculation, gave bond distances around the transition metal atom, which were slightly longer than the experimental ones.[15]

The adopted atom numeration is reported in Fig. 2. Selected computed bond distances, angles and relative energies for the isomers at lower energy are reported in Table 2. In all optimized models of **9**–**11**, theoretical calculations indicate that the *endo-syn-syn* and *exo-syn-syn* conformational isomers are those at lower energy and of those, concerning the Pd–C bond distances, the Pd–C_1 (C_1 being the allyl-carbon atom *trans* to the 2-pyridinyl or the 8-quinolinyl nitrogen atom), are longer than the Pd–C_3 (C_3 being the allyl-carbon atom in *trans* position to nitrogen of the chiral frameworks (*S*)-(+)–2,2′-(2-azapropane-1,3-diyl)-1,1′-binaphthalene) or *trans*-2,5-dimethylpyrrolidinyl. For [Pd(η^3-PhCHCHCHPh)((S_a)-**1**)]$^+$, **9**, the models indicate that the energy difference between the *endo-syn-syn* and the *exo-syn-syn* conformational isomers is low (5.56 kJ), while the energy difference between the *endo-syn-syn* and the *exo-anti-syn* isomers is 21.46 kJ mol^{-1}; the difference between the Pd–C_1 and Pd–C_3 is lower for the *endo-syn-syn* conformational isomer (0.028 Å) than for the *exo-anti-syn* isomer (0.069 Å). In the conformational

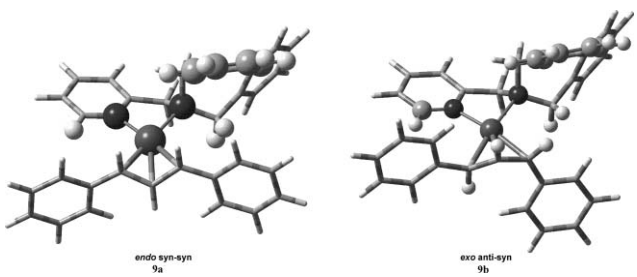

Fig. 6 Minimized structures of the Pd–allyl complex **9** in which is seen the repulsions between the allylic-phenyl group and the CH_2 group of the azepine fragment.

isomers of **9**, the models used clearly show the existence of repulsive interactions between the phenyl-substituent on the terminal allylic carbon atoms and the heterocyclic ring of coordinated (S_a)-**1**. Both the *endo-syn-syn* or *exo-anti-syn* isomers show the pyridinyl *ortho*-hydrogen directed toward the centre of the phenyl-substituent on the allyl carbon in a *cis* position (Fig. 6); the distance between the *ortho*-hydrogen and the C_{pivot} of the phenyl ring of about 2.65 Å indicates a short contact between the pyridinyl-ring and the phenyl-substituent. Also, in the *exo-syn-syn* isomer, we observed the same short contact with a mean value of 2.64 Å.

Likewise, the minimized models indicate repulsive interactions between one $-CH_2-$ of the chiral frameworks (*S*)-(+)–2,2′-(2-azapropane-1,3-diyl)-1,1′-binaphthalene) moiety and the C_{pivot} of the phenyl-substituent on the allyl carbon atom in a *cis* position to azepine nitrogen atom. The distance between the $-CH_2-$ and the C_{pivot} of the phenyl ring was shown to be about 2.68 Å. This short contact interaction contributed to make the palladium–carbon bond (Pd–C_1) in a *trans* position to pyridinyl longer than the one in a *trans* position to the azepine moiety.

Geometry optimization of models for [Pd(η^3-PhCHCHCHPh)((*S*,*S*)-**3**)]$^+$, **10**, and [Pd(η^3-PhCHCHCHPh)((*S*,*S*)-**4**)]$^+$, **11**, indicate the *endo-syn-syn* and *exo-syn-syn* conformational isomers as being more stable and the *exo-anti-syn* as the isomer having stability closer to that of the above-mentioned isomers. For **10** and **11**, the *endo-syn-syn* was observed to be a more stable isomer and the energy difference with respect to the *exo-syn-syn* was estimated as 3.15 and 1.91 kJ mol^{-1} respectively.

It is noteworthy that a *trans*-2,5-dimethylpyrrolidinyl chiral framework was almost perpendicular to the metal coordination plane. In the complexes **10** and **11**, containing the *trans*-2,5-dimethylpyrrolidinyl chiral framework, the (*S*,*S*)-**3** and (*S*,*S*)-**4** coordinated chiral ligands established important repulsive interactions between the allylic phenyl-substituent and the CH_2 and CH of the pyrrolidinyl ring. The distances between the C_{pivot} of the phenyl ring and the CH_2 and CH were about 2.69 Å. In this case, no significant interactions between the allylic phenyl-substituent and the methyl groups were found. In all optimized models, we found a pronounced unsymmetrization in the terminal allyl carbon–palladium distances.

In the compounds **9**–**11**, the computed angle values of N_1–Pd–N_2, N_1–Pd–C_1, N_2–Pd–C_3 and C_1–Pd–C_3 changed in a restricted range, particularly in their more stable conformational isomers *exo-syn-syn* and *endo-syn-syn* (Table 2). There was a significant difference between the N_1–Pd–C_1 and N_2–Pd–C_3 angle values; the larger value of the N_1–Pd–C_1 average angle 108.9° (108.1–110.1°) than the N_2–Pd–C_2 one 104.4° (103.4–105.6°) was the result of the important short contact interactions between the phenyl substituent on the C_1 allyl-carbon atom and the (*S*)-(+)–2,2′-(2-azapropane-1,3-diyl)-1,1′-binaphthalene or *trans*-2,5-dimethylpyrrolidinyl chiral frameworks.

Palladium-catalyzed asymmetric allylic alkylation reactions

We tested the versatility of the chelating C_2-chiral ligands (S_a)-**1**, (*S*,*S*)-**3** and (*S*,*S*)-**4**, in the palladium–allyl catalyzed substitution reaction of 1,3-diphenylallyl acetate with dimethylmalonate (Scheme 1). In accord with the previous results indicating the failure of the cationic complex [Pd(η^3-PhCHCHCHPh)((S_a)-**2**)]CF_3SO_3 synthesis, the ligand (S_a)-**2** did not result in a catalytic process.

Table 3 Allylic alkylation of 1,3-diphenylprop-2-enyl acetate with dimethyl malonate[a]

Entry	Ligand	Solvent	Time/h	Yield[b] (%)	ee[c] (%)
1	(S_a)-**1**	CH_2Cl_2	2.5	96	82 (*S*)
2	(S_a)-**1**	Toluene	2.5	100	82 (*S*)
3	(S_a)-**2**	CH_2Cl_2	No reaction		
4	(*S*,*S*)-**3**	CH_2Cl_2	3	100	6 (*R*)
5	(*S*,*S*)-**4**	CH_2Cl_2	36	58	32 (*R*)

[a] [(η^3-C_3H_5)PdCl]$_2$ (0.0064 mmol), ligand (0.0128 mmol), $H_2C(COOMe)_2$ (2.56 mmol), BSA (2.56 mmol), KOAc (0.06 mmol), CH_2Cl_2[5]. [b] Yield of analytically pure product after column chromatography. [c] Determined by ^{1}H NMR spectroscopy ($CDCl_3$: 0.25 equiv. [Eu(hfc)$_3$]).[5]

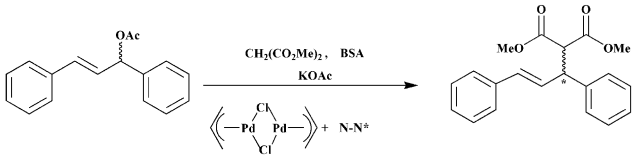

Scheme 1

The product 2-(1,3-diphenylallyl)dimethylmalonate was obtained in a yield and an enantiomeric excess strongly depending on the features of the chiral ligand used in the catalytic process. The best result was obtained using the ligand (S_a)-**1**, in which case, the substitution product of 1,3-diphenyl-2-propenyl acetate with dimethylmalonate was obtained with an enantiomeric excess of 82% (*S*) and a yield of 96% (Table 3, entry 1). Changing the solvent exerted no significant effect either on the yield or the enantiomeric excess (Table 3, entry 2). The (*S*,*S*)-**3** and (*S*,*S*)-**4** ligands afforded the 2-(1,3-diphenylallyl)dimethylmalonate substitution product with a lower enantiomeric excess than (S_a)-**1** ligand; respectively in 6% (*R*), 100%, 32% (*R*), and 58% yield (Table 3, entries 4 and 5). Using the ligand in the (*S*,*S*)-configuration, the 2-(1,3-diphenylallyl)dimethyl-malonate was obtained in the *R* configuration.

Discussion

The different performances of the reported ligands in the catalytic process could be classified in relation to the different sp^3 or sp^2 carbon atom spacer of the ligand arms. In the (S_a)-**1**, and (*S*,*S*)-**3** ligands, the sp^3 carbon atom spacer induces higher flexibility than the sp^2 spacer carbon atom present in (S_a)-**2** and (*S*,*S*)-**4**. The N_1–C(sp^2)–C(sp^2)–N_2 atom arrangement induces rigidity on (S_a)-**2** and (*S*,*S*)-**4**; consequently, their coordination as chelating N-N-ligands to the η^3-diphenylallyl–palladium moiety is not much favourite. The fact that (S_a)-**2** failed to react with [Pd(η^3-PhHCCHCHPh)Cl]$_2$ to give the cationic complex [Pd(η^3-PhHCCHCHPh)((S_a)-**2**)]CF_3SO_3, but it reacts easily with [Pd(η^3-H_2CCHCH_2)Cl]$_2$, in which phenyl-substituents are not present on terminal allylic carbon atoms, to give [Pd(η^3-H_2CCHCH_2)((S_a)-**2**)]CF_3SO_3, **12**, strongly supports the viewpoint that the electronic properties of the chiral framework N-donor atom are not responsible for this behaviour. Moreover, the reaction which utilizes **11** as a catalyst requires an induction time to occur. Differently, the flexibility of the N_1–C(sp^3)–C(sp^2)–N_2 atom arrangement allows

both nitrogen atoms of the (S_a)-**1** and (*S*,*S*)-**3** ligands to easily approach the palladium atom and also to form conformational isomers, which are not of high stability, as for the **9b** isomer of the (S_a)-**1** ligand.

It is a widely proven fact that the enantioselectivity of the allylic substitution reaction process is determined by the regioselectivity of the nucleophilic attack at the terminal allylic carbon atoms.[14] As shown by NMR studies and confirmed by theoretical calculations, in the palladium–diphenyl–allyl catalysts **9–11**, the regioselectivity is mainly induced by the different intra-complex steric hindrances between the *trans*-2,5-dimethylpyrrolidinyl or the (*S*)-(+)–2,2′-(2-azapropane-1,3-diyl)-1,1′-binaphthalene) moieties, contained in the (S_a)-**1**, (*S*,*S*)-**3**, and (*S*,*S*)-**4** ligands, and the phenyl-substituent on the allyl carbon atom in a *cis* position.[12–14] As discussed in the "NMR studies" section and results from Pd–C bond distances deduced by DFT calculations, the *trans*-influence of the N-donor atoms bound to the palladium centre, is not the main factor determining the regioselectivity of the catalytic process. Very indicative of the negligible role of the ligand N-donor atom's power are the computed bond distances Pd–N_1, Pd–N_2, Pd–C_1 and Pd–C_3 average value (Å) for the most stable conformational isomers *exo-syn-syn* and *endo-syn-syn* (the result is practically unchanged considering all the conformational isomers reported in Table 2): **9**: Pd–N_1 2.250, Pd–N_2 2.137, Pd–C_1 2.260, Pd–C_3 2.211; **10**: Pd–N_1 2.259, Pd–N_2 2.129, Pd–C_1 2.285, Pd–C_3 2.217; **11**: Pd–N_1 2.257, Pd–N_2 2.107, Pd–C_1 2.291, Pd–C_3 2.218. The distance of the Pd–C_3 bond, in a *trans* position to the chiral framework N_1, having higher donor power is always shorter than the Pd–C_1 bond distance; the reported data clearly indicate that repulsive interactions between the chiral framework coordinated through N_1-donor atom and the phenyl-substituent at C_1-allylic carbon atom minimizes the electronic effect of the N_1-donor atom. While the Pd–N_2 bond distance discriminates between the pyridinyl- and quinolidinyl ligands, the Pd–N_1 bond distance, the same as Pd–C_1 and Pd–C_3 ones, is nearly unchanged in compounds **9–11**.

The understanding of the origin of the enantioselectivity of the catalytic allylic substitution process requires, in principle, a knowledge of the regioselectivity of the nucleophilic attack at the terminal allylic carbon atoms for each conformational isomers of the catalytic species. Fortunately, the regioselectivity of the nucleophilic attack at terminal allylic carbons is supplied by the ^{13}C NMR spectra, from the chemical shift values of the allylic carbon atoms and, in a more specific way, from the difference between their relative values. The results discussed here clearly prove that structural features of the coordinated chiral ligand, like flexibility or rigidity, are not able to fully explain the experimental data.

In fact, in the catalytic intermediate **9**, the downfield chemical shift of ^{13}C allylic carbon C_1 in the *exo-anti-syn* conformer indicated that it is more suited to nucleophilic attack with respect to the same carbon atom in the other prevalent conformer. ^{13}C NMR spectra indicate that in the *exo-anti-syn* isomer, nucleophilic attack at carbon C_1 is also favoured by the smaller steric hindrance of the closer *S*-binaphthyl fragment (see Fig. 4). The *endo-syn-syn* and the *exo-anti-syn* isomers are involved in an exchange process, and the *exo-anti-syn* conformational isomer is the most reactive towards nucleophilic attack (in the *exo-anti-syn* isomer the difference in the ^{13}C NMR chemical shift of terminal allylic carbon atoms is about 12.0 ppm). The related reaction is faster than the *endo-syn-syn* conformer (Fig. 4) and, occurring under Curtin–Hammett conditions, the *exo-anti-syn* conformational isomer determines the enantioselectivity of the process and the absolute configuration of the substitution product. However, nucleophilic attack at C_1 allylic carbon atoms in the *endo-syn-syn* and in the *exo-anti-syn* isomers, gives 2-(1,3-diphenylallyl)dimethylmalonate in the *S* absolute configuration for both cases; this allows the retrieval of the allylic alkylation reaction product in high enantiomeric excess and in the *S* absolute configuration.

The behaviour of **10**, as a catalyst, is very significant. As expected, the major isomers in solution are *exo-syn-syn*, **10a**, and *endo-syn-syn*, **10b**, which have been suggested to be involved in a fast exchange process, with coalescence at catalytic experimental conditions. It can be assumed that under these conditions, the nucleophile does not distinguish between the two terminal allylic carbons and as a result the catalytic reaction gives the product in low yield with very low enantiomeric excess, even if a more accurate analysis should take into account a comparison between the typical rate of allylic alkylation reaction and that of the dynamic process observed for this system.

Compound **11** contains the more rigid chiral ligand (*S*,*S*)-**4** and allows us to obtain the allylic substitution product only with a very low enantiomeric excess. This contrasts with the fact that (*S*,*S*)-**4** induces the greatest difference observed (comparing conformational isomer which differs only for the coordinated chiral ligand[16]) between th e^{13}C chemical shift values of the terminal allylic carbon atoms, respectively of 4.1 and 3.3 ppm, in the *endo-syn-syn*, **11a**, and *exo-syn-syn*, **11b**, conformational isomers. The comparison of these ^{13}C NMR data with those of the conformational isomers, which are different only for the chelated chiral ligands, indicates that the ligand rigidity enhances the regioselectivity of the nucleophilic attack, more than the ligand flexibility. It is noteworthy that the *endo-syn-syn*, **11a**, and *exo-syn-syn*, **11b** conformational isomers are not involved in an exchange process with each other.

The situation observed for every isomer would reasonably suppose that the (*S*,*S*)-**4** ligand, owing to its rigidity, induces high regioselectivity in allylic carbon nucleophilic attack; consequently, the 2-(1,3-diphenyl-allyl)dimethylmalonate product would have to be obtained with high enantiomeric excess. As a matter of fact, every isomer catalyzes the related process and gives the product with the prevalence of one enantiomer (ee). The observed enantiomeric excess of 2-(1,3-diphenylallyl)dimethylmalonate is the result of a balance between the amounts of 2-(1,3-diphenylallyl)dimethylmalonate, in the *R* and *S* absolute conformation, produced from each catalyst isomer present in solution. The models indicate that the dimethylmalonate nucleophilic attack at C_1 allylic carbon atoms of isomers **11a** and **11b**, should obtain the 2-(1,3-diphenylallyl)dimethylmalonate in the *R* and *S* absolute configuration, respectively. It can reasonably be supposed that, in this case, the low enantiomeric excess can be due to the presence, in solution, of more isomers that give the product in the different absolute configuration.

The results also indicate that rigidity of the 2-pyridinyl and 8-quinolinyl heterocyclic rings containing the nitrogen donor atom also induces repulsive interactions with the substituent on the terminal allylic carbon atom in a *cis*-position, even if to a more minor extent than the chiral N-donor chiral framework. Therefore, this is also a factor determining the regioselectivity of the nucleophilic attack.

It is noteworthy to mention that the metallacycle ring effect is not a factor which influences the process, since all the ligands reported here form a five-membered ring by chelation to the palladium centre.

Conclusions

The rigidity or flexibility features of the coordinated chiral chelating ligands (S_a)-**1**, (S_a)-**2**, (*S*,*S*)-**3** and (*S*,*S*)-**4** do not explain the results obtained in the palladium–allyl catalyzed substitution reaction of 1,3-diphenylallyl acetate with dimethylmalonate. In order to overcome the seeming contradictions that emerge from the results, the characterization of the conformational isomers of the palladium–diphenylallyl catalytic species (at least, occurring under Curtin–Hammett conditions, those in major concentrations) and the identification of exchange processes are indispensable. An indicative knowledge of the amount and of the absolute configuration of the 2-(1,3-diphenylallyl)dimethylmalonate reaction product, for every catalytically active palladium–diphenylallyl conformational isomer present in solution, is of fundamental importance for a reasonable and rigorous explanation about the origin of the observed enantioselectivity of the catalytic product. Therefore, deeper NMR studies and theoretical calculations are indispensable supports to the interpretation of the experimental results and to the reached conclusions in the palladium(II) catalyzed allylic substitution reactions.

Experimental

General methods

All manipulation were carried out under an argon atmosphere using standard Schlenk techniques. Freshly distilled solvents were used throughout and dried by standard procedures. Published methods were used to prepare the compound (2*R*,5*R*)-2,5-hexandiol cyclic sulfate,[17] (S_a)-(+)–2,2′-[2-(methyl-2-pyridyl)-2-azapropane-1,3-diyl]-1,1′-binaphthalene, **1**[7], and [Pd(η^3-PhCH-CHCHPh)(μ-Cl)]$_2$.[18] All other reagents were purchased from Sigma-Aldrich and Strem and were used as supplied. For column chromatography, silica gel 60 (220 ± 440 mesh) and neutral aluminium oxide activity grade 1 (70–290 mesh) purchased from Fluka was used. Optical rotations were obtained with a JASCO P-1010 Automatic Polarimeter in a 1 dm cell; *c* in g per 100 mL. 1D and 2D NMR experiments were carried out using a Bruker AMX R300 spectrometer. ^{1}H NMR spectra were referenced to internal tetramethylsilane. For the **9**–**11** compounds, the resonances of the terminal allylic carbon C_1 and C_3 are reported in Table 1. Standard pulse sequences were employed for phase-sensitive (TPPI method) ^{1}H-2D-NOESY, ^{13}C–^{1}H-correlation (HMQC) studies.[19] Elemental analyses were performed by Redox s.n.c., Cologno Monzese, Milano.

All calculations were carried out using the Gaussian G03W program package.[15] The structures and bonding parameters were computed at the density functional (DFT) B3LYP level of theory, using Becke's exchange functional, which includes the Slater exchange along with corrections involving the gradient of the density[20] and Perdew and Wang's gradient-corrected correlation functional.[21, 22]

Preparations

(S_a)-(−)-2,2′-[(7-Quinolinyl)-2-azapropane-1,3-diyl]-1,1′-binaphthalene (S_a)-2. To a solution of (*S*)-(−)-2,2′-dibromomethyl-1,1′-binaphthalene (400 mg, 0.91 mmol) in anhydrous THF (40 mL) under an inert atmosphere was added 8-aminoquinoline (792 mg, 5.5 mmol). The solution was stirred under reflux for 18 h then cooled to rt. The solution was filtered and the solid residue was washed with THF. The resulting collected solution was concentrated *in vacuo.* The recovered residue was dissolved in $CHCl_3$, washed sequentially with H_2O and brine, and the organic layer was dried over anhydrous Na_2SO_4. The solid residue recovered after evaporation of the solvent was then purified by column chromatography (neutral Al_2O_3; CH_2Cl_2–Et_2O, 85 : 15) affording (S_a)-**2** as a yellow powder. Yield: 82% (315 mg, 0.74 mmol). $[\alpha]^{26}_D = -318.2$ (*c* 1, $CHCl_3$). ^{1}H NMR ($CDCl_3$): δ 8.91 (dd, 1H, ^3J 4 Hz, ^4J 2 Hz, Ar-H), 8.15 (dd, 1H, ^3J 8 Hz, ^4J 2 Hz, Ar-H), 7.91 (dd, 2H, ^3J 8 Hz, Ar-H), 7.88 (d, 2H, ^3J 8 Hz, Ar-H), 7.57 (d, 2H, ^3J 8 Hz, Ar-H), 7.53–7.18 (m, 9H, Ar-H), 6.97 (dd, 1H, ^3J 7 Hz, ^4J 2 Hz, Ar-H), 4.73 (d, 2H, ^3J 12 Hz, CH_2), 4.17 (d, 2H, ^3J 12 Hz, CH_2). Anal. Calcd for $C_{31}H_{22}N_2$ (422.52): C, 88,12; H, 5,25; N, 6,63. Found: C, 88,03; H, 5,37; N, 6,60%.

(*S*,*S*)-(+)-2-(2,5-Dimethylpyrrodin-1-ylmethyl)pyridine (*S*,*S*)-3. 2-Aminomethylpyridine (447 mg, 4.13 mmol) and (2*R*,5*R*)-2,5-hexandiol cyclic sulfate (400 mg, 2.22 mmol) were refluxed in dry THF (10 mL) for 16 h. The resulting precipitate indicated the presence of the Zwitterionic amine–sulfate species. The Schlenk flask was cooled to −78 °C and *n*-butyllithium (1.6 M, 1.53 mL, 2.42 mmol) was added. The mixture was warmed to room temperature and then refluxed for 72 h. Diethyl ether was added to the solution which was then washed with 10% ammonium chloride, water, and brine and extracted into diethyl ether. The extract was dried ($MgSO_4$) and concentrated to yield the crude material. Purification using column chromatography, alumina, hexane–diethyl ether 2 : 1, gave (*S*,*S*)-**3** as a yellow oil. Yield: 75% (320 mg, 1.68 mmol). $[\alpha]^{26}_D = -101.1$ (*c* 1, $CHCl_3$). ^{1}H NMR ($CDCl_3$): δ 8.51 (d, 1H, ^3J 4 Hz, Ar-H), 7.61 (td, 1H, ^3J 8 Hz, ^4J 2 Hz, Ar-H), 7.47 (d, 1H, ^3J 8 Hz, Ar-H), 7.10 (m, 1H, Ar-H), 3.89 (d, 1H, ^2J 14 Hz, CH_2), 3.76 (d, 1H, ^2J 14 Hz, CH_2), 3.08 (m, 2H, CH), 2.01 (m, 2H, CH_2), 1.38 (m, 2H, CH_2), 0.97 (d, 6H, ^3J 7Hz, CH_3). Anal. Calcd for $C_{12}H_{18}N_2$ (190.28): C, 75.74; H, 9.53; N, 14.72. Found: C, 75.78; H, 9.51; N, 14.68%.

(*S*,*S*)-(+)-8-(2,5-Dimethylpyrrodin-1-yl)quinoline (*S*,*S*)-4. 8-Aminoquinoline (595 mg, 4.13 mmol) and (2*R*,5*R*)-2,5-hexandiol cyclic sulfate (400 mg, 2,22 mmol) were refluxed in dry THF (10 mL) for 16 h. The resulting precipitate indicated the presence of the Zwitterionic amine–sulfate species. The Schlenk flask was cooled to −78 °C and *n*-butyllithium (1.6 M, 1.53 mL, 2.42 mmol) was added. The mixture was warmed to room temperature and then refluxed for 72 h. Diethyl ether was added to the solution which was then washed with 10% ammonium chloride, water, and brine and extracted into diethyl ether. The extract was dried ($MgSO_4$) and concentrated to yield the crude material which was purified using column chromatography, alumina, hexane–diethyl ether 2 : 1, to give (*S*,*S*)-**4** as a yellow oil which crystallize on cooling. Yield: 77% (390 mg, 1.72 mmol). $[\alpha]^{26}_D = -220.2$ (*c* 1, $CHCl_3$). ^{1}H NMR ($CDCl_3$): δ 8.85 (dd, 1H, ^3J 4 Hz, ^4J 2 Hz, Ar-H), 8.06 (dd, 1H, ^3J 8 Hz, ^4J 2 Hz, Ar-H), 7.41 (t, 1H, ^3J 8 Hz,

Ar-H), 7.33 (dd, 1H, ^3J 8 Hz, ^4J 4 Hz, Ar-H), 7.29 (dd, 1H, ^3J 8 Hz, ^4J 2 Hz, Ar-H), 7.00 (dd, 1H, ^3J 8 Hz, Ar-H), 4.62 (b, 2H, CH), 2.30 (m, 2H, CH_2), 1.67 (m, 2H, CH_2), 0.95 (b, 6H, CH_3). Anal. Calcd for $C_{15}H_{18}N_2$ (226.32): C, 79.61; H, 8.02; N, 12.38. Found: C, 79.55; H, 8.12; N, 12.36%.

[Pd(N-N*)Cl$_2$] (5–8). The [Pd(N-N*)Cl_2] complexes with N-N* = (S_a)-**1** (**5**), (S_a)-**2** (**6**), (*S*,*S*)-**3** (**7**), (*S*,*S*)-**4** (**8**), were synthesized in the same way with the following procedure.

To a solution of [Pd(benzonitrile)$_2Cl_2$] (20 mg, 52.1 mmol) in CH_2Cl_2 the ligand (62.6 mmol) was added. After the addition the colour of the solution switches from orange to light yellow. After 3 h solvent was removed *in vacuo* and the residue was washed with hexane. Recrystallization from a 3 : 1 ratio of CH_2Cl_2–hexane gave the complex as a yellow solid product.

*[Pd((S$_a$)-**1**)Cl$_2$] (**5**).* Yield: 85% (25 mg, 0.044 mol). ^{1}H NMR ($CDCl_3$): δ 8.97 (dd, 1H, ^3J 6 Hz, ^4J 2 Hz, Ar-H), 8.28 (d, 1H, ^3J 8 Hz, Ar-H), 8.07 (d, 1H, ^3J 8 Hz, Ar-H), 8.00–7.88 (td, 3H, ^3J 8 Hz, ^4J 2 Hz, Ar-H), 7.83 (td, 1H, ^3J 8 Hz, ^4J 2 Hz, Ar-H), 7.72 (d, 1H, ^3J 8 Hz, Ar-H), 7.48 (m, 3H, Ar-H), 7.28 (m, 5H, Ar-H), 5.75 (d, 1H, ^2J 15 Hz, CH_2), 4.83 (d, 1H, ^2J 14 Hz, CH_2), 4.45 (d, 1H, ^2J 14 Hz, CH_2), 4.43 (d, 1H, ^2J 12 Hz, CH_2), 3.64 (d, 1H, ^2J 15 Hz, CH_2), 3.02 (d, 1H, ^2J 12 Hz, CH_2). Anal. Calcd for $C_{28}H_{22}Cl_2N_2Pd$ (563.81): C, 59.65; H, 3.93; N, 4.97. Found: C, 59.61; H, 3.92; N, 4.91%.

*[Pd((S$_a$)-**2**)Cl$_2$] (**6**).* Yield: 81% (25.3 mg, 0.042 mol). ^{1}H NMR ($CDCl_3$): δ 9.65 (dd, 1H, ^3J 5 Hz, ^4J 2 Hz, Ar-H), 8.43 (dd, 1H, ^3J 8 Hz, ^4J 2 Hz, Ar-H), 8.28 (d, 1H, ^3J 8 Hz, Ar-H), 8.08 (dd, 2H, ^3J 8 Hz, ^4J 4 Hz, Ar-H), 8.00 (dd, 2H, ^3J 19 Hz, ^4J 8 Hz, Ar-H), 7.87 (dd, 1H, ^3J 8 Hz, ^4J 2 Hz, Ar-H), 7.63 (dd, 1H, ^3J 5 Hz, Ar-H), 7.56 (t, 1H, ^3J 7 Hz, Ar-H), 7.49–7.40 (m, 5H, Ar-H), 7.31 (t, 1H, ^3J 7 Hz, Ar-H), 7.21 (d, 2H, ^3J 4 Hz, Ar-H), 6.06 (d, 1H, ^2J 14 Hz, CH_2), 4. 94 (d, 1H, ^2J 12 Hz, CH_2), 4.48 (d, 1H, ^2J 14 Hz, CH_2), 4.14 (d, 1H, ^2J 12 Hz, CH_2). Anal. Calcd for $C_{31}H_{22}Cl_2N_2Pd$ (599.85): C, 62.07; H, 3.70; N, 4.67. Found: C, 62.12; H, 3.64; N, 4.61%.

*[Pd((S,S)-**3**)Cl$_2$] (**7**).* Yield: 75% (14.5 mg, 0.039 mol). ^{1}H NMR ($CDCl_3$): δ 9.05 (d, 1H, ^3J 6 Hz, Ar-H), 7.94 (t, 1H, ^3J 8 Hz, Ar-H), 7.65 (d, 1H, ^3J 8 Hz, Ar-H), 7.40 (t, 1H, ^3J 7 Hz, Ar-H), 4.54 (d, 1H, ^2J 15 Hz, CH_2), 4.12 (m, 1H, CH), 3.62 (d, 1H, ^2J 15 Hz, CH_2), 3.03 (m, 1H, CH), 2.30 (m, 1H, CH_2), 2.11 (m, 1H, CH_2), 1.93 (d, 3H, ^3J 7 Hz, CH_3), 1.89 (m, 1H, CH_2), 1.63 (m, 1H, CH_2), 1.61 (d, 3H, ^3J 7 Hz, CH_3). Anal. Calcd for $C_{12}H_{18}Cl_2N_2Pd$ (367.61): C, 39.21; H, 4.94; N, 7.62. Found: C, 39.30; H, 4.92; N, 7.57%.

*[Pd((S,S)-**4**)Cl$_2$] (**8**).* Yield: 78% (16.4 mg, 0.041 mol). ^{1}H NMR ($CDCl_3$): δ 9.62 (dd, 1H, ^3J 5 Hz, ^4J 1 Hz, Ar-H), 8.43 (dd, 1H, ^3J 8 Hz, ^4J 2 Hz, Ar-H), 7.91 (dd, 1H, ^3J 7 Hz, ^4J 2 Hz, Ar-H), 7.78–7.70 (m, 2H, Ar-H), 7.58 (dd, 1H, ^3J 8 Hz, ^4J 5 Hz, Ar-H), 5.70 (m, 1H, CH), 3.76 (m, 1H, CH), 2.73 (m, 1H, CH_2), 2.27 (m, 1H, CH_2), 2.12 (m, 1H, CH_2), 2.19 (d, 3H, ^3J 7 Hz, CH_3), 1.97 (m, 1H, CH_2), 1.06 (d, 3H, ^3J 7 Hz, CH_3). Anal. Calcd for $C_{15}H_{18}Cl_2N_2Pd$ (403.64): C, 44.63; H, 4.49; N, 6.94. Found: C, 44.60; H, 4.53; N, 6.91%.

[Pd(η^3-PhCHCHCHPh)(N-N*)]CF_3SO_3 (9–11). The following procedure for the preparation of **11** is representative and the [Pd-(η^3-PhCHCHCHPh)(N-N*)]CF_3SO_3 complexes (N-N*) = (S_a)-**1** (**9**), (*S*,*S*)-**3** (**10**), (*S*,*S*)-**4** (**11**), were synthesized in a similar manner. This complex was synthesized by reaction of [Pd(η^3-PhCHCHCHPh)(μ-Cl)]$_2$ (0.020 g, 0.030 mmol) with the ligand (N-N*) (0.06 mmol) in CH_2Cl_2 (25 ml) at room temperature. After 1 h $AgCF_3SO_3$ (0.015 g, 0.06 mmol) was added and the mixture was stirred for 10 min. The suspension was filtered through a pad of Celite, the solvent evaporated *in vacuo* except for a few millilitres, and the product precipitated with hexane. Recrystallized from CH_2Cl_2–hexane in a 3 : 1 ratio, a yellow powder was obtained.

*[Pd(η^3-PhCHCHCHPh)((S$_a$)-**1**)]CF_3SO_3 (**9**).* Yield: 75% (38 mg, 0.045 mmol). ^{1}H NMR ($CDCl_3$) at 298 K: *endo-syn-syn* δ 8.23 (d, 1H, ^3J 8 Hz, Ar-H), 8.10 (d, 1H, ^3J 8 Hz, Ar-H), 8.06–7.88 (m, 4H, Ar-H), 7.86 (t, 1H, ^3J 8 Hz, Ar-H), 7.62 (t, 1H, ^3J 8 Hz, Ar-H), 7.48 (d, 1H, H_{opy}), 7.47–7.23 (m, 10H, Ar-H), 7.24 (m, 6H, Ar-H), 7.05 (t, 1H, ^3J 8 Hz, Ar-H), 6.80 (t, 1H, ^3J 8 Hz, Ar-H), 6.48 (dd, 1H, ^2J 12 Hz, CH_2, 2), 4.95 (d, 1H, ^2J 12 Hz, CH_2, 3), 4.72 (d, 1H, ^2J 15 Hz, CH_2, 4a), 4.33 (d, 1H, ^2J 12 Hz, CH_2, 1), 4.08 (d, 1H, ^2J 12 Hz, CH_2, 5a), 3.70 (d, 1H, ^2J 15 Hz, CH_2, 4b), 3.35 (d, 1H, ^2J 14 Hz, CH_2, 6a), 2.89 (d, 1H, ^2J 12 Hz, CH_2, 5b), 2.35 (d, 1H, ^2J 14 Hz, CH_2, 6b); *exo-anti-syn*: δ 8.26 (br, 1H, Ar-H), 8.07 (br, 1H, Ar-H), 8.04–7.86 (m, 4H, Ar-H), 7.85 (br, 1H, Ar-H), 7.59 (br, 1H, Ar-H), 7.53 (d, 1H, H_{opy}), 7.48–7.21 (m, 10H, Ar-H), 7.20 (m, 6H, Ar-H), 7.02 (br, 1H, Ar-H), 6.80 (t, 1H, ^3J 8 Hz, Ar-H), 6.35 (br, 1H, CH_2, 2), 5.47 (br, 1H, CH_2, 4a), 5.38 (br, 1H, CH_2, 1), 4.84 (br, 1H, CH_2, 3), 4.27 (br, 1H, CH_2, 5a), 3.69 (br, 1H, CH_2, 4b), 3.44 (br, 1H, CH_2, 6a), 2.95 (br, 1H, CH_2, 5b), 2.64 (br, 1H, CH_2, 6b). Conductivity value of 89 μS in methanol solution, using a 5 × 10^{-4}–1 × 10^{-4} molar concentration. Anal. Calcd for $C_{44}H_{35}F_3N_2O_3PdS$ (835.24): C, 63.27; H, 4.22; N, 3.35. Found: C, 64.51; H, 3.98; N, 3.41%.

*[Pd(η^3-PhCHCHCHPh)((S,S-**3**)]CF_3SO_3 (**10**).* Yield: 76% (29.2 mg, 0.046 mmol). ^{1}H NMR ($CDCl_3$) at 223 K: *exo-syn-syn* δ 7.80–7.61 (m, 8H, Ar-H), 7.56 (d, 1H, H_{opy}), 7.51–7.37 (m, 6H, Ar-H), 6.52 (dd, 1H, ^2J 12 Hz, CH_2, 2), 4.88 (d, 1H, ^2J 12 Hz, CH_2, 3), 4.84 (d, 1H, ^2J 12 Hz, CH_2, 1), 4.48 (d, 1H, ^2J 15 Hz, CH_2, 4a), 3.73 (d, 1H, ^2J 15 Hz, CH_2, 4b), 2.73 (m, 1H, CH, 5), 2.28 (m, 1H, CH, 6), 2.00 (m, 1H, CH_2, 7a), 1.65 (m, 1H, CH_2, 8a), 1.44 (d, 3H, ^3J 7 Hz, CH_3), 1.28 (m, 1H, CH_2, 8b), 1.17 (m, 1H, CH_2, 7b), 1.01 (d, 3H, ^3J 7 Hz, CH_3); *endo-syn-syn*: δ 7.80–7.61 (m, 8H, Ar-H), 7.16 (d, 1H, H_{opy}), 7.51–7.37 (m, 6H, Ar-H), 6.58 (dd, 1H, ^2J 12 Hz, CH_2, 2), 4.79 (d, 1H, ^2J 12 Hz, CH_2, 3), 4.65 (d, 1H, ^2J 12 Hz, CH_2, 1), 3.94 (d, 1H, ^2J 15 Hz, CH_2, 4a), 3.78 (d, 1H, ^2J 15 Hz, CH_2, 4b), 3.09 (m, 1H, CH, 6), 2.43 (m, 1H, CH, 5), 2.14 (m, 1H, CH_2, 7a), 1.57 (d, 3H, ^3J 7 Hz, CH_3), 1.40 (m, 1H, CH_2, 7b), 1.28 (m, 1H, CH_2, 8a), 1.24 (m, 1H, CH_2, 8b), 0.70 (d, 3H, ^3J 7 Hz, CH_3). Conductivity value of 83 μS in methanol solution, using a 5 × 10^{-4}–1 × 10^{-4} molar concentration. Anal. Calcd for $C_{28}H_{31}F_3N_2O_3PdS$ (639.04): C, 52.63; H, 4.89; N, 4.38. Found: C, 53.68; H, 4.86; N, 4.42%.

*[Pd(η^3-PhCHCHCHPh)((S,S)-**4**)]CF_3SO_3 (**11**).* Yield: 82% (33.2 mg, 0.049 mmol). ^{1}H NMR ($CDCl_3$) at 298 K: *endo-syn-syn* δ 8.35 (d, 1H, ^3J 4 Hz, Ar-H), 8.33 (t, 1H, ^3J 6 Hz, Ar-H), 7.92–7.45 (m, 9H, Ar-H), 7.79 (d, 1H, H_{opy}), 7.22–7.13 (m, 4H, Ar-H), 6.57 (dd, 1H, ^2J 12 Hz, CH_2, 2), 5.14 (d, 1H, ^2J 12 Hz, CH_2, 3), 5.10 (d, 1H, ^2J 12 Hz, CH_2, 1), 3.69 (m, 1H, CH, 5), 2.17 (m, 1H, CH, 6), 1.91 (m, 1H, CH_2, 7a), 1.67 (d, 3H, ^3J 7 Hz, CH_3), 1.61 (m, 1H, CH_2, 8a), 1.38 (m, 1H, CH_2, 8b), 0.70 (d, 3H, ^3J 7 Hz, CH_3), 0.49 (m, 1H, CH_2, 7b); *exo-syn-syn*: δ 8.92 (d, 1H, ^3J 4 Hz, Ar-H), 8.35 (t, 1H, ^3J 6 Hz, Ar-H), 7.92–7.45 (m, 9H, Ar-H), 7.48 (d, 1H, H_{opy}), 7.22–7.13 (m, 4H, Ar-H), 6.64 (dd, 1H, ^2J 12 Hz, CH_2, 2), 5.19 (d, 1H, ^2J 12 Hz, CH_2, 3), 5.08 (d, 1H, ^2J 12 Hz, CH_2, 1), 4.67 (m,

1H, CH, 6), 3.55 (m, 1H, CH, 5), 2.10 (m, 1H, CH_2, 7a), 1.52 (m, 1H, CH_2, 7b), 1.36 (m, 1H, CH_2, 8a), 1.15 (d, 3H, ^3J 7 Hz, CH_3), 1.05 (m, 1 H, CH_2, 8b), 0.98 (d, 3 H, ^3J 7 Hz, CH_3). Conductivity value of 80 μS in methanol solution, using a 5×10^{-4}–1×10^{-4} molar concentration. Anal. Calcd for $C_{31}H_{31}F_3N_2O_3PdS$ (675.07): C, 55.15; H, 4.63; N, 4.15. Found: C, 55.20; H, 4.64; N, 4.18%.

[Pd(η³-CH_2CHCH_2)((S_a)-2)]CF_3SO_3 (12). This complex was synthesized by reaction of $[Pd(\eta^3\text{-}C_3H_5)(\mu\text{-}Cl)]_2$ (0.010 g, 0.027 mmol) with the ligand (S_a)-**2** (0.023 g, 0.065 mmol) in CH_2Cl_2 (5 ml) at room temperature. After 1 h $AgCF_3SO_3$ (0.014 g, 0.055 mmol) was added and was stirred for 10 min. The suspension was filtered through a pad of Celite, the solvent evaporated *in vacuo* except for a few millilitres, and the product precipitated with hexane. Recrystallized from CH_2Cl_2–hexane in a 3 : 1 ratio, a light pink powder was obtained. Yield: 70% (13.7 mg, 0.019 mol). ^{1}H NMR ($CDCl_3$): δ 9.28 (d, 1 H, ^3J 5 Hz, Ar-H), 8.51 (d, 1H, ^3J 8 Hz, Ar-H), 8.17 (t, 2H, ^3J 9 Hz, Ar-H), 8.07 (d, 2H, ^3J 8 Hz, Ar-H), 8.01 (d, 1H, ^3J 8 Hz, Ar-H), 7.95 (d, 1H, ^3J 8 Hz, Ar-H), 7.82 (dd, 1H, ^3J 8 Hz, Ar-H), 7.59 (m, 5H, Ar-H), 7.37 (m, 4H, Ar-H), 5.83 (b, 1H, CH_2), 5.05 (d, 1H, CH), 5.00 (b, 2H, CH_2), 4.86 (b, 2H, CH_2), 4.46 (b, 1H, CH_2), 4.30 (d, 1H, CH_2), 3.37 (d, 1H, CH_2). Conductivity value of 82 μS in methanol solution, using a 5×10^{-4}–1×10^{-4} molar concentration. Anal. Calcd for $C_{35}H_{27}F_3N_2O_3PdS$ (719.08): C, 58.46; H, 3.78; N, 3.90. Found: C, 58.50; H, 3.75; N, 3.91%.

Palladium-catalyzed allylic alkylation

General procedure. In a 30 ml Schlenk tube equipped with magnetic stirring bar, under argon, $[Pd(\eta^3\text{-}C_3H_5)(\mu\text{-}Cl)]_2$ (2.34 mg, 0.0064 mmol) was treated with the N-N* ligand (0.0128 mmol) in CH_2Cl_2 (0.7 ml). The solution was degassed (three freeze–thaw cycles) and stirred for 0.5 h. After this period, to the solution was sequentially added the 1,3-diphenyl-1-acetoxypropene (323 mg, 1.28 mmol), dimethylmalonate (338.2 mg, 2.56 mmol), *N*,*O*-bis(trimethylsilyl)acetamide (520.8 mg, 2.56 mmol), and KOAc (6 mg, 0.06 mmol) and then degassed (three freeze–thaw cycles). The reaction was monitored by TLC (eluent: hexane–AcOEt 3 : 1) and, at the end, the mixture was diluted with Et_2O and extracted with two portions of ice-cold saturated aqueous NH_4Cl solution. The solution was dried ($MgSO_4$) and evaporated *in vacuo*; the residue was purified by column chromatography (silica gel, 4 × 30 cm, hexane–AcOEt 3 : 1) to afford the product as a colourless oil. The optical purity was determinated by NMR using paramagnetic shift reagent [Eu(hfc)$_3$]. Assignment of the absolute configuration was made by the sign of the optical rotation.

Acknowledgements

This work was supported by Ministero dell'Istruzione, dell'Università e della Ricerca (MIUR-Rome; PRIN Nos 2005035123).

Notes and references

1 (*a*) C. G. Frost, J. Howarth and J. M. J. Williams, *Tetrahedron: Asymmetry*, 1992, **3**, 1089; (*b*) B. M. D. Trost and L. Van Vranken, *Chem. Rev.*, 1996, **96**, 395; (*c*) B. M. D. Trost and C. Lee, in *Catalytic Asymmetric Synthesis*, ed. I. Ojima, Wiley-VCH, New York, 2nd edn, 2000, p. 593; (*d*) I. Ojima, *Catalytic Asymmetric Synthesis*, VCH Publishers, New York, 1993; (*e*) R. Noyori, *Asymmetric Catalysis in Organic Synthesis*, John Wiley & Sons, New York, 1994; (*f*) B. M. D. Trost and T. R. Verhoeven, *J. Am. Chem. Soc.*, 1976, **98**, 630; (*g*) B. M. D. Trost and T. R. Verhoeven, *J. Am. Chem. Soc.*, 1978, **100**, 3435; (*h*) G. A. Molander, J. P. Burke and P. J. Carroll, *J. Org. Chem.*, 2004, **69**, 8062; (*i*) O. G. Mancheño, J. Priego, S. Cabrera, R. G. Arrayás, T. Llamas and J. C. Carretero, *J. Org. Chem.*, 2003, **68**, 3680.

2 (*a*) A. Pfaltz, *Acc. Chem. Res.*, 1993, **26**, 339; (*b*) U. Leutenegger, G. Umbricht, C. Fahrni, P. von Matt and A. Pfaltz, *Tetrahedron*, 1992, **48**, 2143; (*c*) P. G. Andersson, A. Harden, D. Tanner and P. O. Norrby, *Chem.–Eur. J.*, 1995, **1**, 12; (*d*) B. M. Trost and I. Hachiya, *J. Am. Chem. Soc.*, 1998, **120**, 1104; (*e*) H. Kubota, M. Nakajima and K. Koga, *Tetrahedron Lett.*, 1993, **34**, 8135; (*f*) K. Nordström, E. Macedo and C. Moberg, *J. Org. Chem.*, 1997, **62**, 1604; (*g*) P. Gamez, B. Dunjic, F. Fache and M. Lemaire, *J. Chem. Soc., Chem. Commun.*, 1994, 1417; (*h*) J. M. Canal, M. Gómez, F. Jiménez, M. Rocamora, G. Muller, E. Duñach, D. Franco, A. Jiménez and F. H. Cano, *Organometallics*, 2000, **19**, 966; (*i*) M. Gómez, S. Jansat, G. Muller, M. A. Maestro and J. M. Saavedra, *Organometallics*, 2002, **21**, 1077; (*j*) M. Svensson, U. Bremberg, K. Hallman, I. Csöregh and C. Moberg, *Organometallics*, 1999, **18**, 4900; (*k*) M. Gómez, S. Jansat, G. Muller, M. A. Maestro, J. M. Saavedra, M. Font-Bardía and X. Solans, *J. Chem. Soc., Dalton Trans.*, 2001, 1432.

3 (*a*) G. Helmchen and A. Pfaltz, *Acc. Chem. Res.*, 2000, **33**, 336; (*b*) J. M. Brown, D. I. Hulmes and P. J. Guiry, *Tetrahedron*, 1994, **50**, 4493; (*c*) P. E. Blöchl and A. Togni, *Organometallics*, 1996, **15**, 4125; (*d*) G. Helmchen, S. Kudis, P. Sennhenn and H. Steinhagen, *Pure Appl. Chem.*, 1997, **69**, 513; (*e*) P. S. Pregosin and G. Trabesinger, *J. Chem. Soc., Dalton Trans.*, 1998, 727; (*f*) G. Helmchen, *J. Organomet. Chem.*, 1999, **576**, 203; (*g*) M. Widhalm, U. Nettekoven, H. Kalchhauser, K. Mereiter, M. J. Calhorda and V. Felix, *Organometallics*, 2002, **21**, 315; (*h*) O. G. Bondarev, S. E. Lyubinov, A. A. Shiryaev, N. E. Kadilnikov, V. A. Davankov and K. N. Gavrilov, *Tetrahedron: Asymmetry*, 2002, **13**, 1587; (*i*) R. Hilgraf and A. Pfaltz, *Synlett*, 1999, **11**, 1814; (*j*) K. Selvakumar, M. Valentini, M. Wörle, P. S. Pregosin and A. Albinati, *Organometallics*, 1999, **18**, 1207; (*k*) A. J. Blacker, M. L. Clarke, M. S. Loft, M. F. Mahon, M. E. Humphries and J. M. J. Williams, *Chem.–Eur. J.*, 2000, **6**, 353; (*l*) R. Prétôt and A. Pfaltz, *Angew. Chem., Int. Ed.*, 1998, **37**, 323; (*m*) C. J. Martin, D. J. Rawson and J. M. J. Williams, *Tetrahedron: Asymmetry*, 1998, **9**, 3723.

4 (*a*) See for example: T. Hayashi, A. Yamamoto, Y. Ito, E. Nishioka, H. Miura and K. Yanagi, *J. Am. Chem. Soc.*, 1989, **111**, 6301; (*b*) W. Zhang, T. Hirao and I. Ikeda, *Tetrahedron Lett.*, 1996, **37**, 4545.

5 (*a*) See for example: B. M. Trost and D. L. Van Vranken, *Angew. Chem., Int. Ed. Engl.*, 1992, **31**, 228; (*b*) B. M. Trost, B. Breit, S. Peukert, J. Zambrano and J. W. Ziller, *Angew. Chem., Int. Ed. Engl.*, 1995, **34**, 2386; (*c*) M. Widhalm, P. Wimmer and G. Klintschar, *J. Organomet. Chem.*, 1996, **523**, 167; (*d*) A. Saitoh, M. Misawa and T. Morimoto, *Tetrahedron: Asymmetry*, 1999, **10**, 1025; (*e*) D. Zhao and K. Ding, *Org. Lett.*, 2003, **5**, 1349.

6 T. Mecca, S. Superchi, E. Giorgio and C. Rosini, *Tetrahedron: Asymmetry*, 2001, **12**, 1225.

7 (*a*) H. Kubota and K. Koga, *Heterocycles*, 1996, **42**, 543; (*b*) K. Warnmark, R. Stranne, M. Cernerud, I. Terrien, F. Rahm, K. Nordstrom and C. Moberg, *Acta Chem. Scand.*, 1998, **7**, 961; (*c*) J. A. Sweet, J. M. Cavallari, W. A. Price, J. W. Ziller and D. V. McGrath, *Tetrahedron: Asymmetry*, 1997, **8**, 207.

8 The basicity of the N-donor atom chiral framework in the (S_a)-**1** and (S_a)-**2** ligands can be correlated with that of dialkylsubstituted azepine type compounds, while in the (*S*,*S*)-**3** and (*S*,*S*)-**4** ligands with that of dialkylsubstituted pyrrolidine type compounds. The pK_a values for dialkylsubstituted azepine and dialkylsubstituted pyrrolidine are *ca.* 9 and 10, respectively. The pK_a value for pyridine and quinoline are very close (*ca.* 5).

9 (*a*) G. Calabrò, D. Drommi, G. Bruno and F. Faraone, *Dalton Trans.*, 2004, **81**; (*b*) C. G. Arena, D. Drommi and F. Faraone, *Tetrahedron: Asymmetry*, 2000, **11**, 2765; (*c*) C. G. Arena, D. Drommi and F. Faraone, *Tetrahedron: Asymmetry*, 2000, **11**, 4753.

10 The structure of **8** was also confirmed by X-ray diffraction: G. Bottari, G. Brancatelli, M. Saporita, D. Drommi, F. Nicolò and F. Faraone, work in progress. The compound [Pd(CH_3)Cl((S_a)-**2**)], similar to **6**, was also characterized by X-ray diffraction analysis:; B. Milani, F. Amoroso, M. R. Axet, E. Zangrando, D. Drommi, M. Saporita and F. Faraone, private communication.

11 Nomenclature note: the structures *endo*- or *exo*- are defined if the central allyl proton is down or up with respect to the coordination plane having an sp^2 or sp^3 N_1 nitrogen atom (quinolinyl or pyridinyl moiety) on the left side (see Fig. 2). According to ref. 18(*b*), the sequence numbering of the allyl part starts with C_1 *cis* to N_1, C_2 for the central carbon, and C_3 *cis* to N_2. Consequently the first geometric descriptor, *syn* or *anti*, refers to the configuration of phenyl allylic substituents at C_1 and C_3 with respect to C_2.

12 (*a*) P. S. Pregosin and R. Salzmann, *Coord. Chem. Rev.*, 1996, **155**, 35; (*b*) S. K. Mandal, G. A. N. Gowda, S. S. Krishnamurthy, C. Zheng, S. Li and N. S. Hosmane, *Eur. J. Inorg. Chem.*, 2002, 2047; (*c*) S. K. Mandal, G. A. N. Gowda, S. S. Krishnamurthy and M. Nethaji, *Dalton Trans.*, 2003, 1016.; (*d*) S. K. Mandal, G. A. N. Gowda, S. S. Krishnamurthy, C. Zheng, S. Li and N. S. Hosmane, *J. Organomet. Chem.*, 2003, **22**, 676; (*e*) U. Burckhardt, D. Drommi and A. Togni, *Inorg. Chim. Acta*, 1999, **296**, 183.

13 (*a*) J. Sprinz, M. Kiefer, G. Helmchen, M. Reggelin, G. Huttner and O. L. Walter Zsolnai, *Tetrahedron Lett.*, 1994, **35**, 1523; (*b*) C. Breutel, P. S. Pregosin, R. Salzmann and A. Togni, *J. Am. Chem. Soc.*, 1994, **116**, 4067; (*c*) B. M. Trost, G. M. Schroeder and J. Kristensen, *Angew. Chem., Int. Ed.*, 2002, **18**, 41; (*d*) J. V. Allen, S. J. Coote, G. J. Dawson, G. C. Frost, C. J. Martin and J. M. Williams, *J. Chem. Soc., Perkin Trans. 1*, 1994, 2065; (*e*) A. Chesney, M. R. Bryce, R. W. J. Chubb, A. S. Batsanov and J. A. K. Howard, *Tetrahedron: Asymmetry*, 1997, **8**, 2337; (*f*) H. Steinhagen, M. Reggelin and G. Helmchen, *Angew. Chem., Int. Ed. Engl.*, 1997, **36**, 2108; (*g*) G. C. Lloyd-Jones and S. C. Stephen, *Chem.–Eur. J.*, 1998, **4**, 2539; (*h*) B. M. Trost and F. D. Toste, *J. Am. Chem. Soc.*, 1999, **121**, 4545; (*i*) H. Eichelmann and H. J. Gais, *Tetrahedron: Asymmetry*, 1995, **3**, 643.

14 (*a*) K. Selvakumar, M. Valentini, P. S. Pregosin and A. Albinati, *Organometallics*, 1999, **18**, 4591; (*b*) P. S. Pregosin, R. Salzmann and A. Togni, *Organometallics*, 1995, **14**, 842; (*c*) P. Dierkes, S. Ramdeehul, L. Barloy, A. De Cian, J. Fischer, P. C. J. Kamer, P. W. N. M. van Leeuwen and J. A. Osborne, *Angew. Chem., Int. Ed.*, 1998, **37**, 3116; (*d*) P. Dierkes, S. Ramdeehul, R. Aguado, P. C. J. Kamer, P. W. N. M. van Leeuwen and J. A. Osborne, *Angew. Chem., Int. Ed.*, 1998, **37**, 3118; (*e*) H. Hoarau, J.-C. Daran Ait-Haddou, D. Cramaliere and G. G. A. Balavoine, *Organometallics*, 1999, **18**, 4718.

15 M. J. Frisch, G. W. Trucks, H. B. Schlegel, P. M. W. Gill, B. G. Johnson, M. A. Robb, J. R. Cheeseman, T. Keith, G. A. Petersson, J. A. Montgomery, K. Raghavachari, M. A. AlLaham, V. G. Zakrzewski, J. V. Ortiz, J. B. Foresman, J. Cioslowski, B. B. Stefanov, A. Nanayakkara, M. Challacombe, C. Y. Peng, P. Y. Ayala, W. Chen, M. W. Wong, J. L. Andres, E. S. Replogle, R. Gomperts, R. L. Martin, D. J. Fox, J. S. Binkley, D. J. Defrees, J. Baker, J. P. Stewart, M. Head-Gordon, C. Gonzalez and J. A. Pople, *GAUSSIAN 03*, Gaussian Inc., Pittsburgh, PA, 2003.

16 The differences between the ^{13}C chemical shift values of the terminal allylic carbon atoms can be significantly compared, and utilized as a measure of the coordinated ligand capability to induce regioselectivity in the nucleophilic attack at allylic carbon atoms, only when the conformational isomers are the same except for the coordinated chiral ligand. Therefore, the value of 12.0 ppm, found in the *exo-anti-syn* isomer of **9b**, is not indicative of a more regioselectivity induction in the nucleophilic attack than **11a** and **11b** due to the fact that these latter compounds contain a rigid framework *vs*. the flexible ligands present in the former **9** species.

17 M. J. Burk, J. E. Feaster, W. A. Nugent and R. L. Harlow, *J. Am. Chem. Soc.*, 1993, **115**, 10125.

18 (*a*) P. Von Matt, G. C. Lloyd-Jones, A. B. E. Midinis, A. Pfaltz, L. Macko, M. Neuburger, M. Zehnder and P. S. Pregosin, *Helv. Chim. Acta*, 1995, **78**, 265; (*b*) A. Togni, U. Burckhardt, V. Gramlich and P. S. Pregosin, *J. Am. Chem. Soc.*, 1996, **118**, 1031.

19 V. SklenaÁr, H. Miyashiro, G. Zon, H. T. Miles and A. Bax, *FEBS Lett.*, 1986, **208**, 94.

20 A. D. Becke, *Phys. Rev. A*, 1988, **38**, 3098.

21 K. Burke, J. P. Perdew, Y. Wang, in *Electronic Density Functional Theory: Recent Progress and New Directions*, ed. J. F. Dobson, G. Vignale and M. P. Das, Plenum, New York, 1998 and references therein.

22 J. P. Perdew, K. Burke and Y. Wang, *Phys. Rev. B: Condens. Matter*, 1996, **54**, 16533.